

# RG-K KY Transferred Polarization

## RG-K Overview

- Acquired Nov. 29- Dec. 20, 2018
- 7.5 GeV with FT-ON:
  - run 5681-5870
  - 10.77 mC,  $P_b=85\%$ ,  $T=+100\%$
- 6.5 GeV with FT-OFF:
  - run 5874-6000
  - 18.23 mC,  $P_b=85\%$ ,  $T=+100\%$

## Motivation


- Understand reaction mechanism
- Probe dynamics of  $q\bar{q}$  string-breaking
- Add insight structure of  $N^*$  states
- Confirm new  $N^*$  states "seen" in KY photoproduction data

Carman, Joo, Mokeev, FBS 61, 29 (2020)

Analysis work nearly done - aiming to call for Working Group review by August - this talk updates progress since March CLAS meeting

# RG-K KY P' Next Steps

Plan as presented at my CLAS Collaboration presentation in March 2021

- ✓ 1. Finalize single-dimensional analysis ( $Q^2$ ,  $W$ ,  $\cos \theta_k^*$ )
- ✓ 2. Work to advance multi-dimensional analysis
- ✓ 3. Quantify systematic uncertainties
- ✓ 4. Continue to develop complete analysis notes for review
- ✓ 5. Work with theorists for model curves
- ✓ 6. Prepare draft of paper - Phys. Rev. C target
7.  Aim for review by end of summer 2021



Next steps: internal RG-K review starting in mid-June and then finish all work to start review by the end of July

# Documentation

All associated analysis documents quite mature

## RG-K General Analysis Note

### CLAS12 RG-K Analysis Note Overview and Procedures

Daniel S. Carman  
Thomas Jefferson National Accelerator Facility, Newport News, VA 23606, USA

Annalisa D'Angelo, Lucilla Lanza  
INFN, Sezione di Roma Tor Vergata, 00133 Rome, Italy

François-Xavier Ghid  
University of Connecticut, Storrs, CT 06269, USA

For the RG-K Run Group

\* Run Group Contact: Annalisa D'Angelo - annalisa.dangelo@roma2.infn.it

#### Abstract

This write-up includes information related to the RG-K dataset acquired in Dec. 2018, details processing and trains for the physics skins outputs, and an overview of the data quality determined after reworking. This note also includes general information on the standard RG-K analysis cuts and an full set of Moller measurements of the electron beam polarization.

1

## RG-K P' Analysis Note

### Precision Beam-Recoil Transferred Polarization in $K^+Y$ Electroproduction in the Nucleon Resonance Region

D.S. Carman, Jefferson Laboratory

V.I. Mokeev, Jefferson Laboratory

A. D'Angelo, INFN, Sezione di Roma Tor Vergata, Università di Roma Tor

L. Lanza, INFN, Sezione di Roma Tor Vergata

(Dated: May 24, 2021)

This write-up includes the analysis details and systematic uncertainty evaluation associated with the extraction of the beam-recoil transferred polarization observables for the exclusive  $p(e, e'K^+)A$  and  $p(e, e'K^+)N$  reactions from the RG-K dataset acquired at beam energies of 6.5 GeV and 7.5 GeV. For this analysis, the  $K^+$  final state is reconstructed with the  $K^+$  and  $p$  in both Forward Detector Central Detector of CLAS12. The data span momentum transfers from 0.3-4.5 GeV<sup>2</sup> and invariant energy from threshold to  $W=2.4$  GeV, while spanning the full center-of-mass angular range of the  $K^+$ .

rgk-tpol-note.tex

## Event Generator Note

### genKYandOnePion Event Generator

V. Khramov,<sup>1,2</sup> V. Mokeev,<sup>2</sup> D.S. Carman,<sup>2</sup>

<sup>1</sup> University of Connecticut, Storrs, Connecticut 06269

<sup>2</sup> Shublyun Nuclear Physics Institute, 118009 Moscow, Russia and

<sup>3</sup> Thomas Jefferson National Accelerator Facility, Newport News, Virginia 23606

(Dated: May 24, 2021)

This note details the basis for the genKYandOnePion event generator using CLAS KY electroproduction data and shows comparisons of the event generator with the data. In addition the range of applicability of the generator is detailed and instructions for its usage either in a stand-alone mode or within the CLAS12 Open Science Grid portal. The code location in the JeffersonLab github repository is provided along with instructions for compiling the code.

## Physics Paper - PRC

Phys. Rev. C

### Precision Beam-Recoil Transferred Polarization in $K^+Y$ Electroproduction in the Nucleon Resonance Region

D.S. Carman,<sup>1</sup> A. D'Angelo,<sup>2,3</sup> L. Lanza,<sup>2</sup> V.I. Mokeev,<sup>1</sup>

(CLAS Collaboration)

<sup>1</sup> Thomas Jefferson National Accelerator Facility, Newport News, Virginia 23606

<sup>2</sup> INFN, Sezione di Roma Tor Vergata, 00133 Rome, Italy and

<sup>3</sup> Università di Roma Tor Vergata, 00133 Rome, Italy

(Dated: April 25, 2021)

Beam-recoil transferred polarizations for the exclusive electroproduction of  $K^+A$  and  $K^+N$  final states from a proton target have been measured using the CLAS12 spectrometer at Jefferson Laboratory. The measurements have been completed at beam energies of 6.5 GeV and 7.5 GeV and span the range of four-momentum transfer  $Q^2$  from 0.3-4.5 GeV<sup>2</sup> and invariant energy  $W$  from 1.6-2.4 GeV, while spanning the full center-of-mass angular range of the  $K^+$ . These new data extend the available hyperon polarization measurements available from CLAS in a similar kinematic range but from a significantly larger dataset. For the first time in  $K^+Y$  electroproduction these data allow measurements with uncertainties approaching those for the available photoproduction measurements from CLAS. These data represent an important addition to the available world data to better understand the reaction mechanisms in strangeness production processes and to further understand the spectrum and structure of excited nucleon states to gain insight into the strong interaction in the regime of non-perturbative dynamics.

PACS numbers: 13.60.Le, 14.20.Gb, 13.30.Eg, 11.80.Et

Keywords: Strangeness production, polarization observables, excited nucleon structure, strong QCD

#### I. INTRODUCTION

Over the past decade significant progress has been realized in mapping out the spectrum of excited nucleon ( $N^*$ ) states and understanding their structure based on data from exclusive meson photo- and electroproduction. These detailed studies hold the key to gain insight into the nature of the strong interaction dynamics that govern these systems [1, 2, 3].

Based mainly on exclusive meson electroproduction data acquired with the CLAS12 detector in Hall B at Jefferson Laboratory (JLab), the nucleon resonance electroproduction amplitudes, i.e. the  $\gamma N^*$  electrocouplings, have become available for most  $N^*$  states in the mass range up to 1.8 GeV for photon virtualities  $Q^2$  up to  $\sim 5$  GeV<sup>2</sup> [4]. These data offer unique information on the strong interaction in the regime of large QCD running coupling, the so-called strong QCD (sQCD) regime that are responsible for the generation of these  $N^*$  states with different quantum numbers and distinctively different structural features as bound systems of quarks and gluons. See Refs. [5, 6] for two recent reviews of the field.

Furthermore, an essential requirement to better understand sQCD dynamics, in particular, the approximate symmetries that underlie  $N^*$  generation, is to map out their spectrum of excited states. Both constituent quark models and lattice QCD approaches predict many more  $N^*$  states than have been unraveled from analysis of the experimental data with a rich spectrum of states predicted and expected in the mass range above 1.8 GeV. This has come to be known as the "missing" resonance problem and the existence of these higher mass excited nucleon states [6].

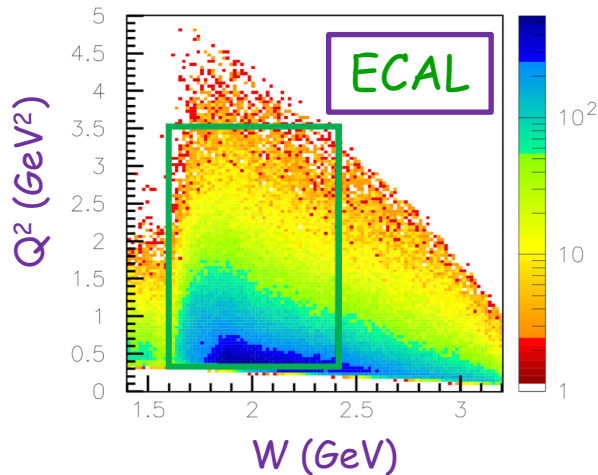
The recent progress in understanding the structure of the nucleon excited states has mainly been provided by advanced analyses of the CLAS data for exclusive electroproduction of the  $\pi^+n$ ,  $\pi^+p$ , and  $\pi^0p$  channels from a proton target. However, recent advances in the exploration of the  $N^*$  spectrum are based on the publication of high-precision data on the exclusive production of  $K^+A$  and  $K^+N$  based on CLAS photoproduction datasets [7-11]. Nine new baryon states have been recently discovered within global multi-channel analyses of the exclusive photoproduction data with a decisive impact from the aforementioned CLAS  $K^+A$  and  $K^+N$  photoproduction results [6, 12]. Through advanced analyses that include cross sections and, in particular, polarization observables from the strangeness channels, our understanding of the  $K^+Y$  channels has expanded significantly. Table I (taken from Ref. [12]) shows a comparison of the current Particle Data Group listings for a dozen  $N^*$  and  $\Delta^*$  states in the mass range up to 2.2 GeV compared to the listings from just a decade ago. For most of these states the addition of the  $K^+Y$  channels has played a key role [12]. Note that the  $K^+A$  and  $K^+N$  channels are important to consider separately. Although the two ground-state hyperons have the same  $u/d$  valence quark content, they have different isospin ( $I=0$  for  $\Lambda$  and  $I=1/2$  for  $\Sigma^0$ ), so that  $N^*$  states of  $I=1/2$  can decay to  $K^+A$ , but  $\Delta^*$  states cannot. Because both  $N^*$  and  $\Delta^*$  resonances can couple to the  $K^+N$  final state, the hyperon final state selection constitutes an isospin filter.

The CLAS  $\gamma p \rightarrow K^+Y$  ( $Y=\Lambda, \Sigma$ ) datasets based on high statistics experiments have allowed for precision measurements with fine binning in the relevant ( $W, \cos\theta_{c.m.}$ ) kinematic phase space. These data have

# Particle Identification

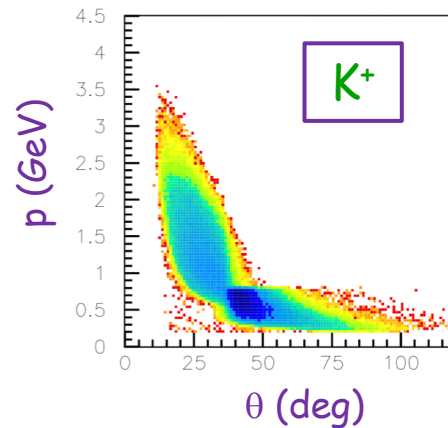
electrons

Cut	Value
Track Status	$2000 \leq \text{abs}(\text{STATUS}) < 4000$
Event Builder PID	11
$p_e$	$1.0 < p_e < p_{beam}$ GeV
$TOF_e$	$21 < TOF_e < 26$ ns
$v_z$	$-10 \leq v_z^e \leq 2$ cm
ECAL Sampling Fraction	$\pm 3.5\sigma$
ECAL Fiducial Cut	7 cm edge cut on $U, V, W$
$\pi^-$ contamination	$E_{ECAL}/p_e < -0.84 * E_{PCAL}/p_e + 0.17$
DC Fiducial Cuts	on



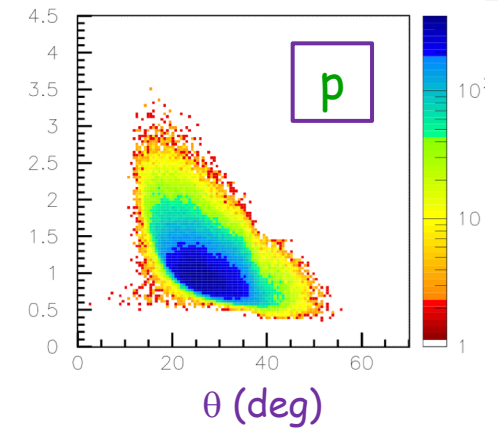
Forward Detector

Cut	Value
Track status	$2000 \leq  \text{STATUS}  < 4000$
$q$	$\neq 0$
$p_h$	$[0.4:p_{beam}]$ GeV
$\beta_h$	$[0.4:1.1]$
Event Builder PID	$\pm 211, \pm 321, \text{ or } \pm 2212$
$TOF_h$	$[20:55]$ ns ( $q > 0$ ), $[20:35]$ ns ( $q < 0$ )
$v_z$	$[-10:2]$ cm ( $K^+$ candidates)
DC Fiducial Cuts	on



hadrons

Cut	Value
Track status	$ \text{STATUS}  \geq 4000$
$q$	$\neq 0$
$p_h$	$[0.2:3.0]$ GeV
$\beta_h$	$[0.2:1.1]$
Event Builder PID	$\pm 211, \pm 321, \text{ or } \pm 2212$
$TOF_h$	$[0.5:4.0]$ ns
$v_z$	$[-10:2]$ cm ( $K^+$ candidates)
Duplicate FD/CD hadron removal	on



Central Detector

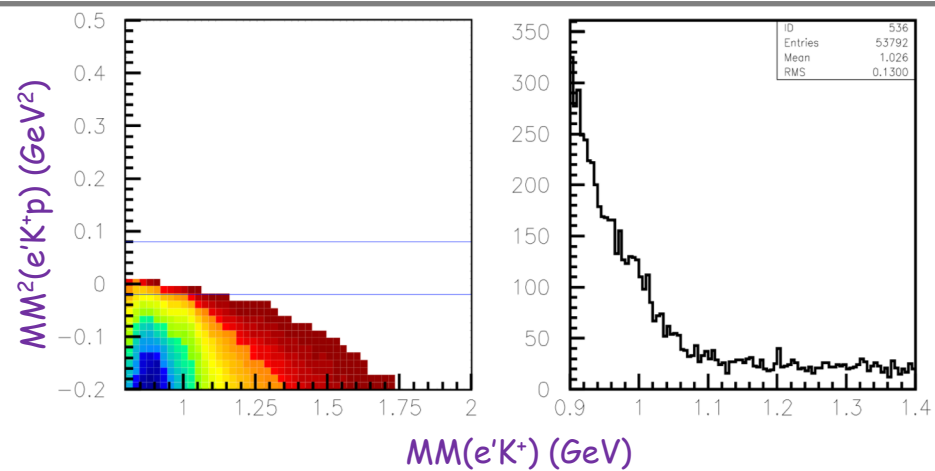
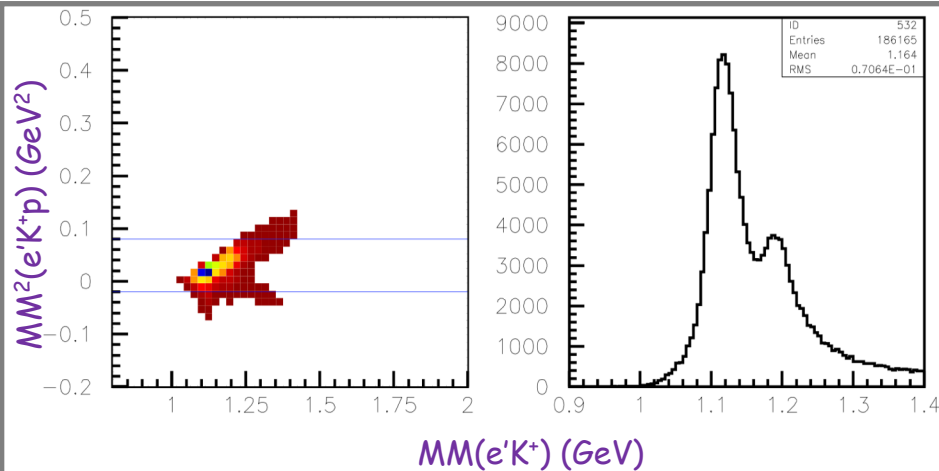
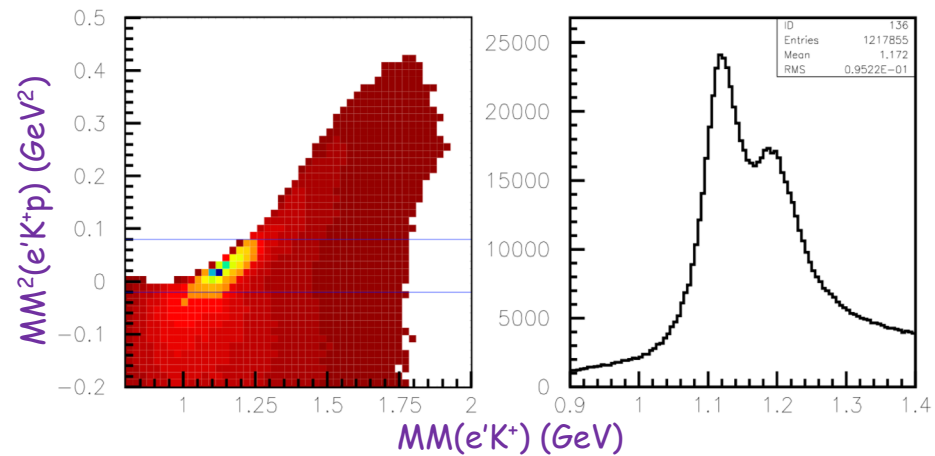
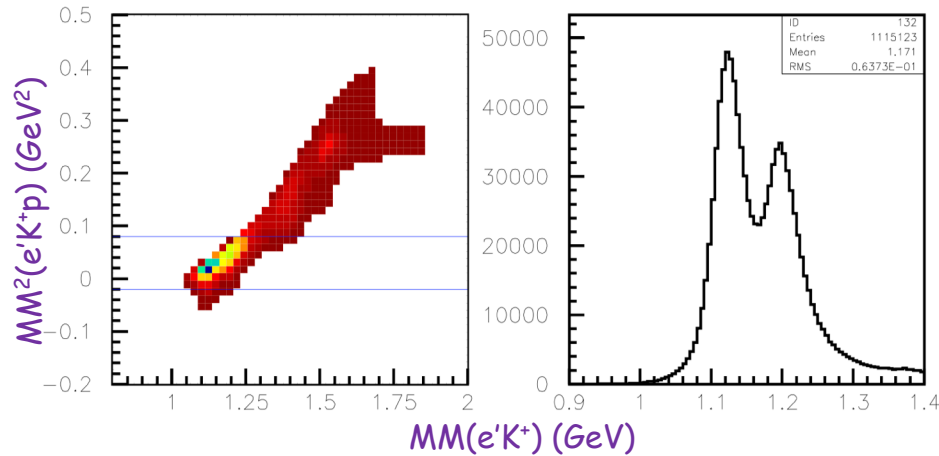


# e'K<sup>+</sup>p Topologies

## Favored Topologies

K<sup>+</sup> forward, p forward

K<sup>+</sup> central, p forward

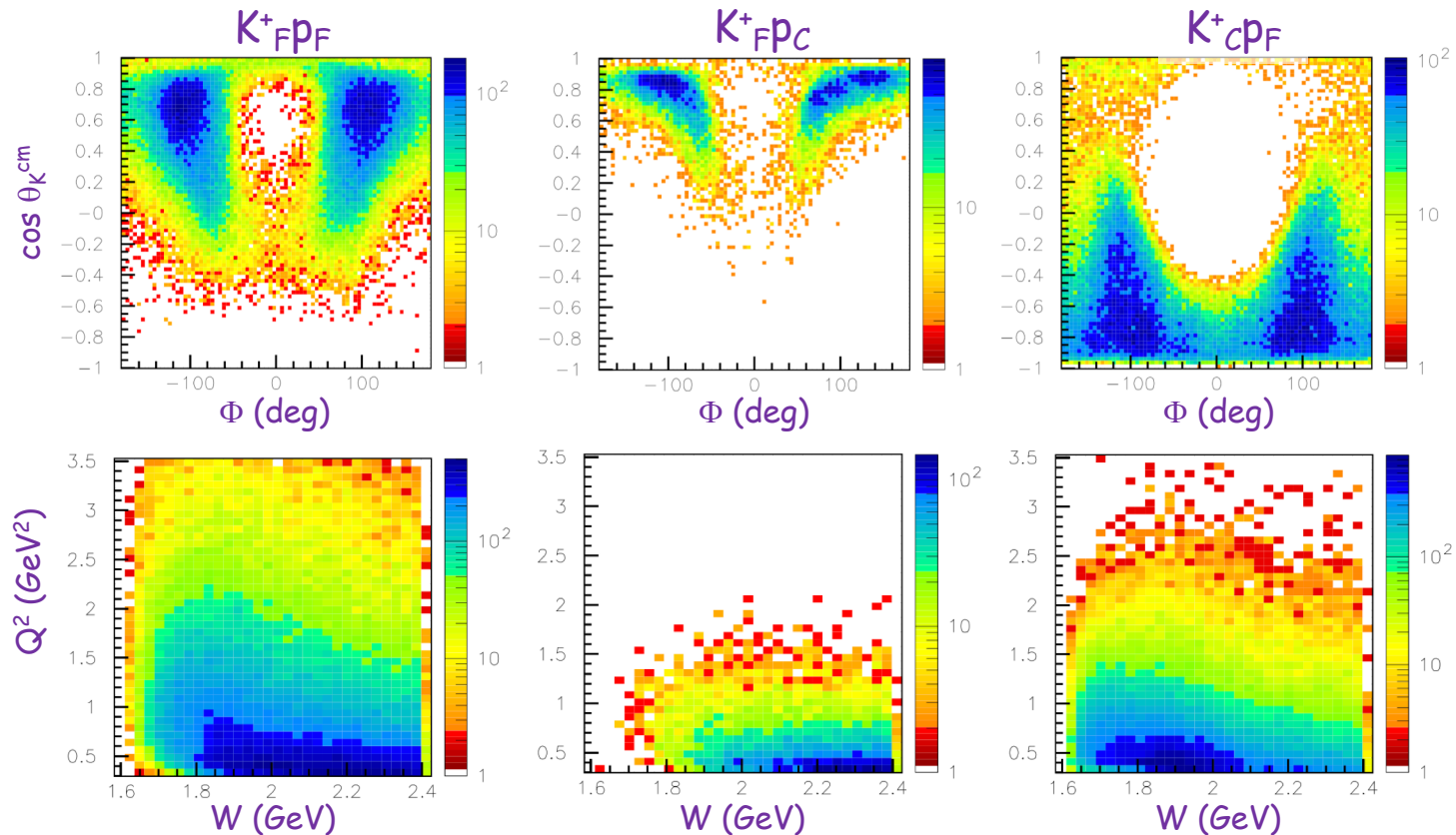


K<sup>+</sup> forward, p central

K<sup>+</sup> central, p central

## Unfavored Topologies

# KY Event Reconstruction



## Strategy:

- Sum 3 topologies together after elec pcorr and bin-by-bin  $MM(e'K^+)$  corrections to put hyperons at their PDG masses separately for each topology
- Perform independent analysis by the Rome Group to extract polarization
- Compare results for different  $Kp$  hadronic topologies
- Compare against existing CLAS data at 5.754 GeV

# Analysis Details

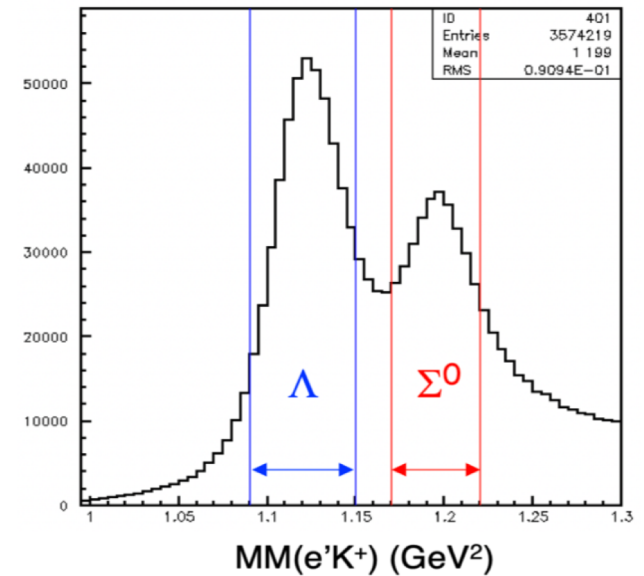
## 1D Binning Sort

Dependence	Range	Bin Size
$Q^2$	0.3 - 1.5 GeV <sup>2</sup>	0.1 GeV <sup>2</sup>
	1.5 - 2.5 GeV <sup>2</sup>	0.2 GeV <sup>2</sup>
	2.5 - 3.1 GeV <sup>2</sup>	0.3 GeV <sup>2</sup>
	3.1 - 3.5 GeV <sup>2</sup>	0.4 GeV <sup>2</sup>
	3.5 - 4.5 GeV <sup>2</sup>	1.0 GeV <sup>2</sup>
$W$	1.6 - 2.4 GeV	25 MeV
$\cos \theta_K^*$	-1 $\rightarrow$ 1	0.08

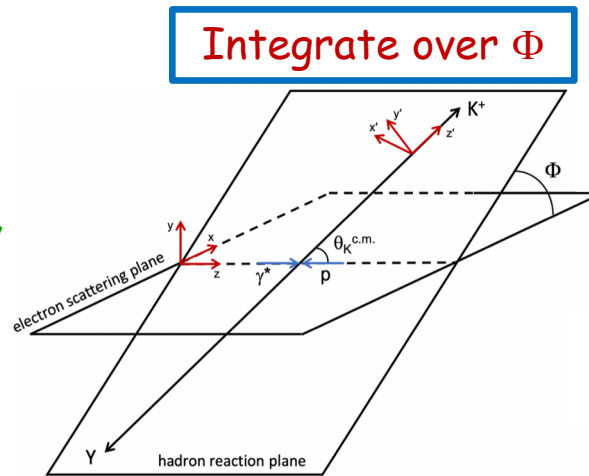
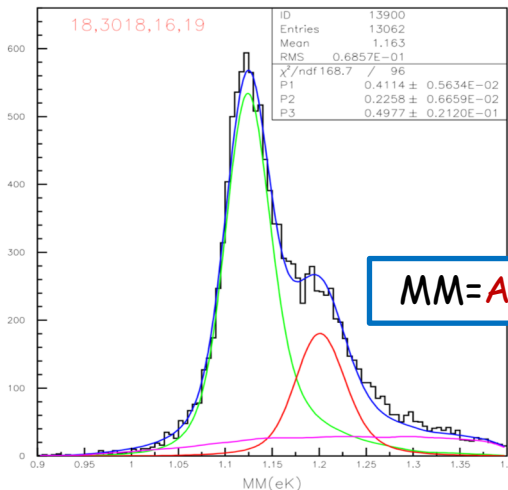
## 3D Binning Sort

Variable	Bin Choices
$Q^2$	0.3 - 0.9 GeV <sup>2</sup> , 0.9 - 3.5 GeV <sup>2</sup>
$W$	1.6 - 2.4 GeV in 80 MeV bins
$\cos \theta_K^*$	-1 $\rightarrow$ 1 in 0.5 bins

## Hyperon Analysis Regions



Template fit:  $\Lambda$ ,  $\Sigma^0$  from MC,  
2 $\pi$  bck from data



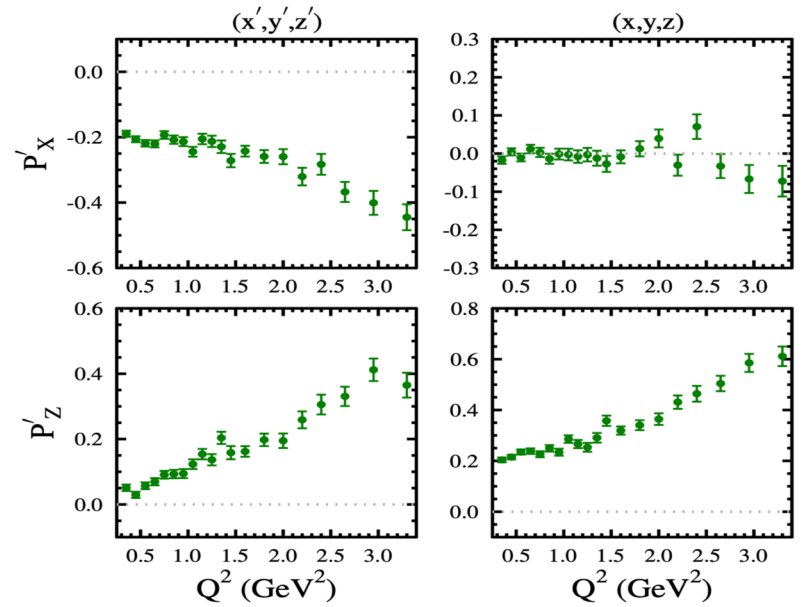
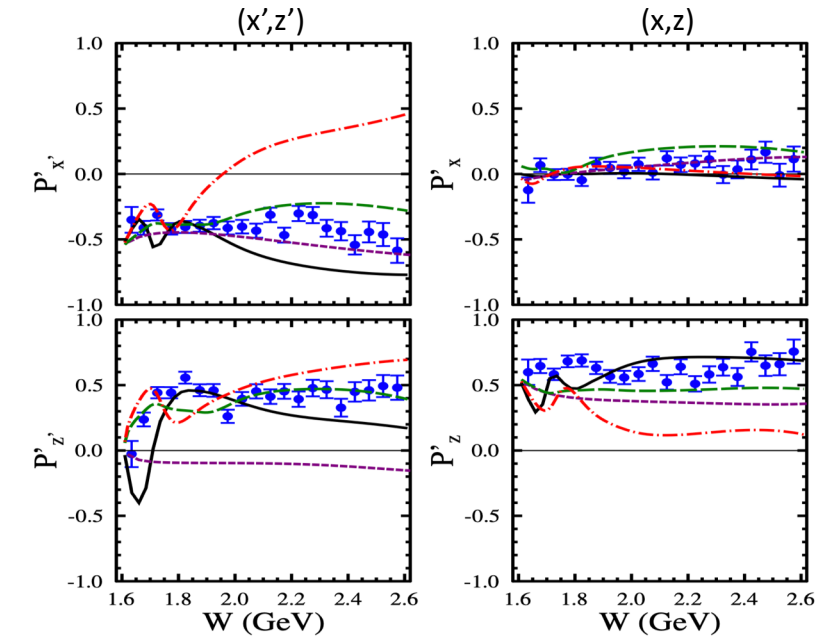
$$A_{meas} = \frac{(N_{\Lambda}^+ + N_{\Sigma}^+ + N_B^+) - (N_{\Lambda}^- + N_{\Sigma}^- + N_B^-)}{N_{\Lambda} + N_{\Sigma} + N_B}$$

$$= \alpha P_b P'_{meas} \cos \theta_P^{RF}$$

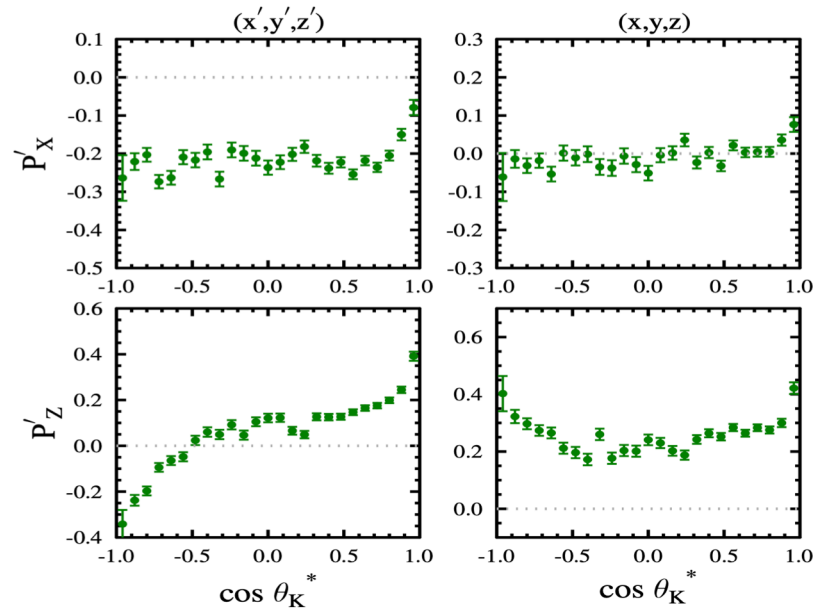
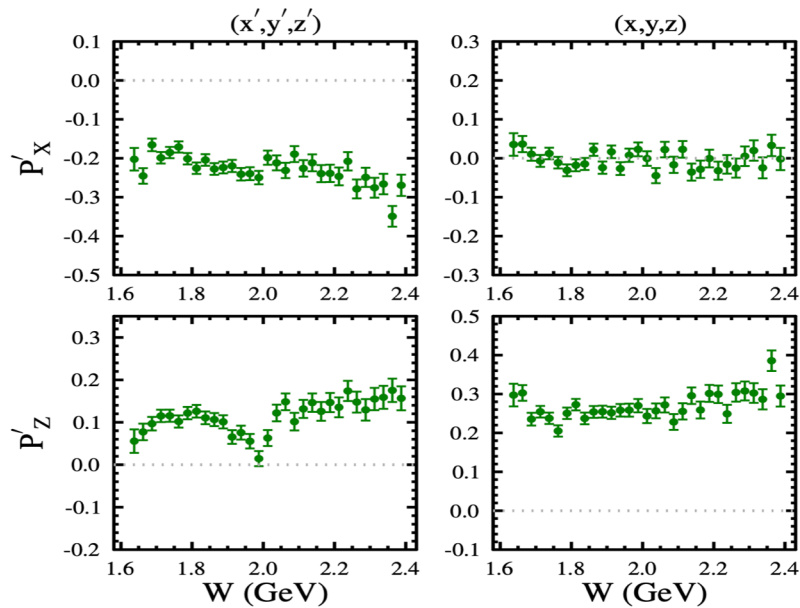
$$P'_{\Lambda} = P'_{meas} (1 + F_{\Sigma} + F_B) - \nu_{\Sigma} P'_{\Sigma} F_{\Sigma}$$

# Beam-Recoil $\Lambda$ Transferred Polarization

D.S. Carman et al., PRC79, 065205 (2009)



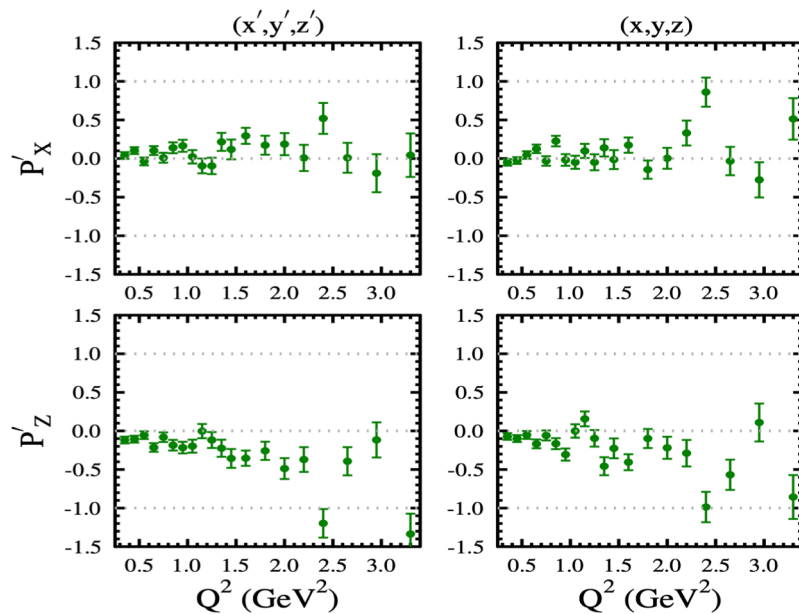
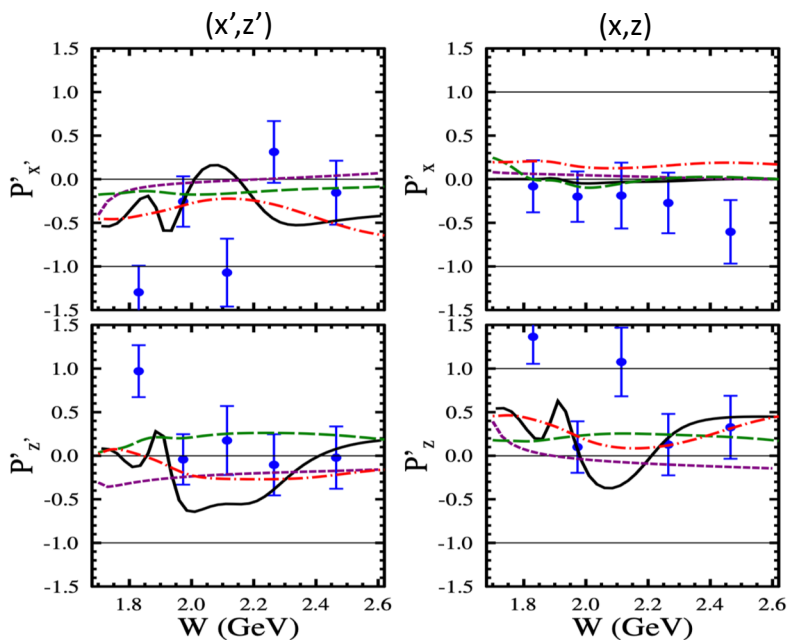
6.5 GeV



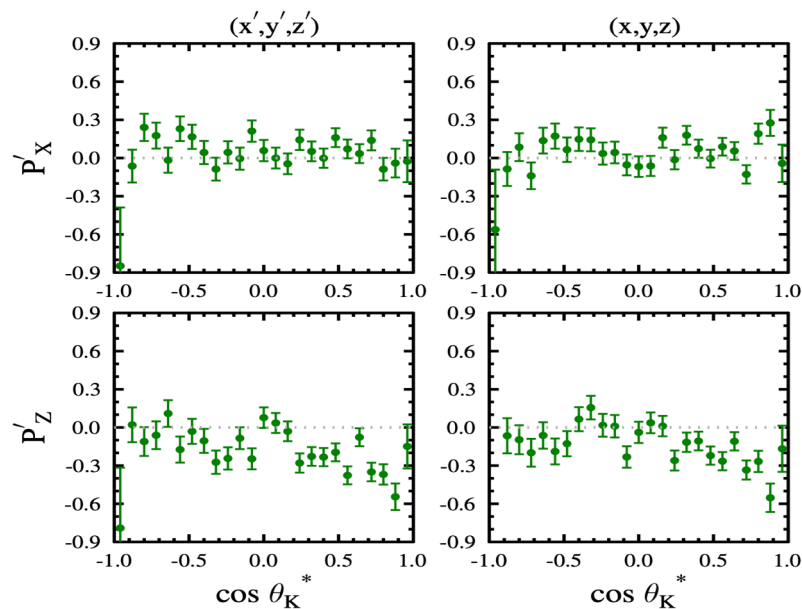
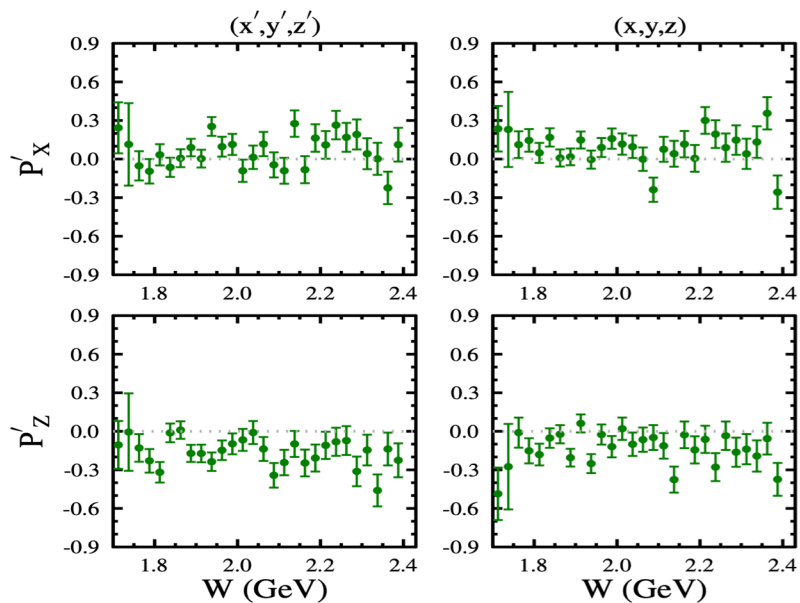
# Beam-Recoil $\Sigma^0$ Transferred Polarization

CLAS e1-6 @ 5.754 GeV

D.S. Carman et al., PRC79, 065205 (2009)

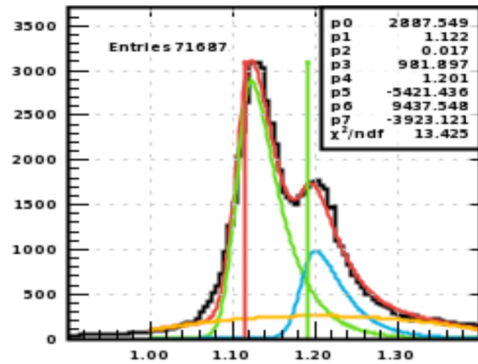


6.5 GeV



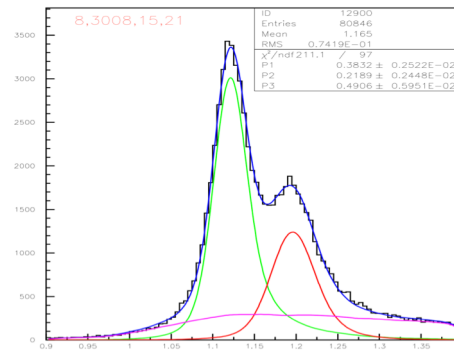
# Beam-Recoil $\Lambda$ Transferred Polarization

Rome



MM(e'K<sup>+</sup>)

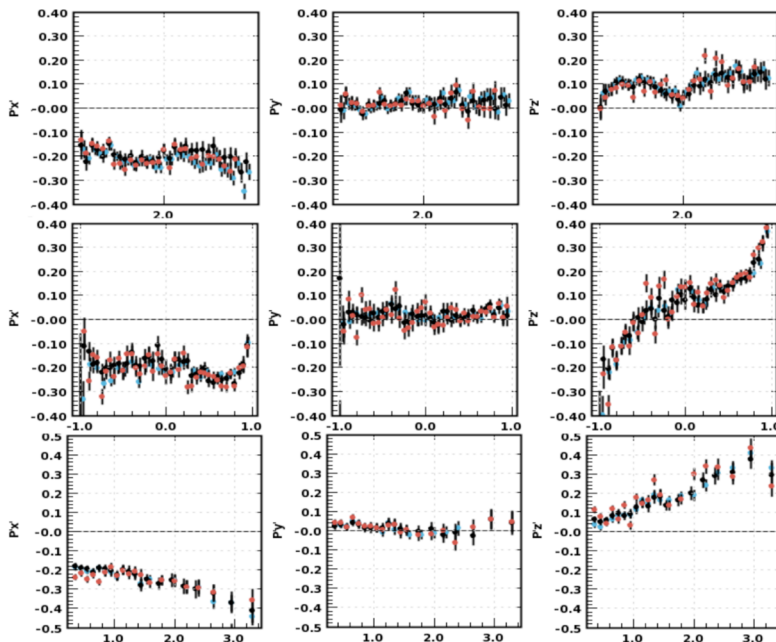
nominal



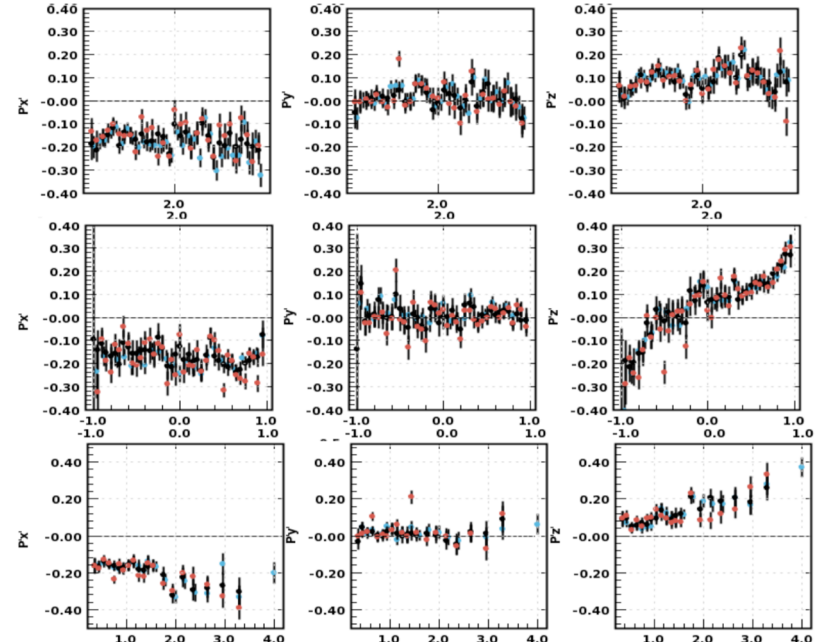
MM(e'K<sup>+</sup>)

6.535 GeV

7.546 GeV



(x',y',z')



Nominal results, Rome approach, Rome cross-check of nominal results



# Systematic Uncertainties

## Categories:

1. Polarization Extraction
2. Beam-Related Factors
3. Acceptance Function
4. Background Contributions

$$\langle P \rangle = \sqrt{\frac{\sum_{i=1}^n \frac{[P_i^{nom} - P_i^{alt}]^2}{(\delta P_i)^2}}{\sum_{i=1}^n \frac{1}{(\delta P_i)^2}}},$$


$$(\delta P_i)^2 = (\delta P_i^{nom})^2 + (\delta P_i^{alt})^2$$



- **SYS1:**  $\cos \theta_p^{RF}$  bin size
- **SYS2:** fiducial cuts tight vs. loose
- **SYS3:** acceptance correction on vs. off
- **SYS4:** background function P2 vs.  $2\pi$
- **SYS5:** ratio vs. asymmetry approach
- **SYS6:**  $P'_y$  component
- **SYS7:**  $P'$  from itop1, itop2, itop3
- **SYS8:** MM( $e^+K^+$ ) cuts loose vs. nom. vs. tight
- **SYS9:** polarization of background events
- **SYS10:** Nominal vs. Rome approach for  $P'$  extraction

Category	Contribution	Systematic Uncertainty
Polarization Extraction	Functional Form	0.005
	Bin Size	0.004
Beam Related Factors	Beam Polarization	3.0%
Acceptance Function	Fiducial Cut Form	0.006
Background Contributions	Analysis Region	0.011 ( $\Lambda$ ), 0.059 ( $\Sigma^0$ ) 1D bins
		0.021 ( $\Lambda$ ), 0.120 ( $\Sigma^0$ ) 3D bins
<b>&lt;Total Systematic Uncertainty&gt;</b>		0.014 $\oplus$ 3% ( $\Lambda$ ), 0.060 $\oplus$ 3% ( $\Sigma^0$ ) 1D bins
		0.023 $\oplus$ 3% ( $\Lambda$ ), 0.120 $\oplus$ 3% ( $\Sigma^0$ ) 3D bins

# RG-K KY P' - The Road Ahead

1. Finish work on systematic uncertainty studies
2. Finish draft of the analysis note
3. Complete internal RG-K review of analysis note
4. Continue to work on paper
5. Work with theorists for model predictions
6. Complete work on general RG-K analysis note
7.  Aim for W.G. review by August 2021



Much more detail on RG-K KY page at:

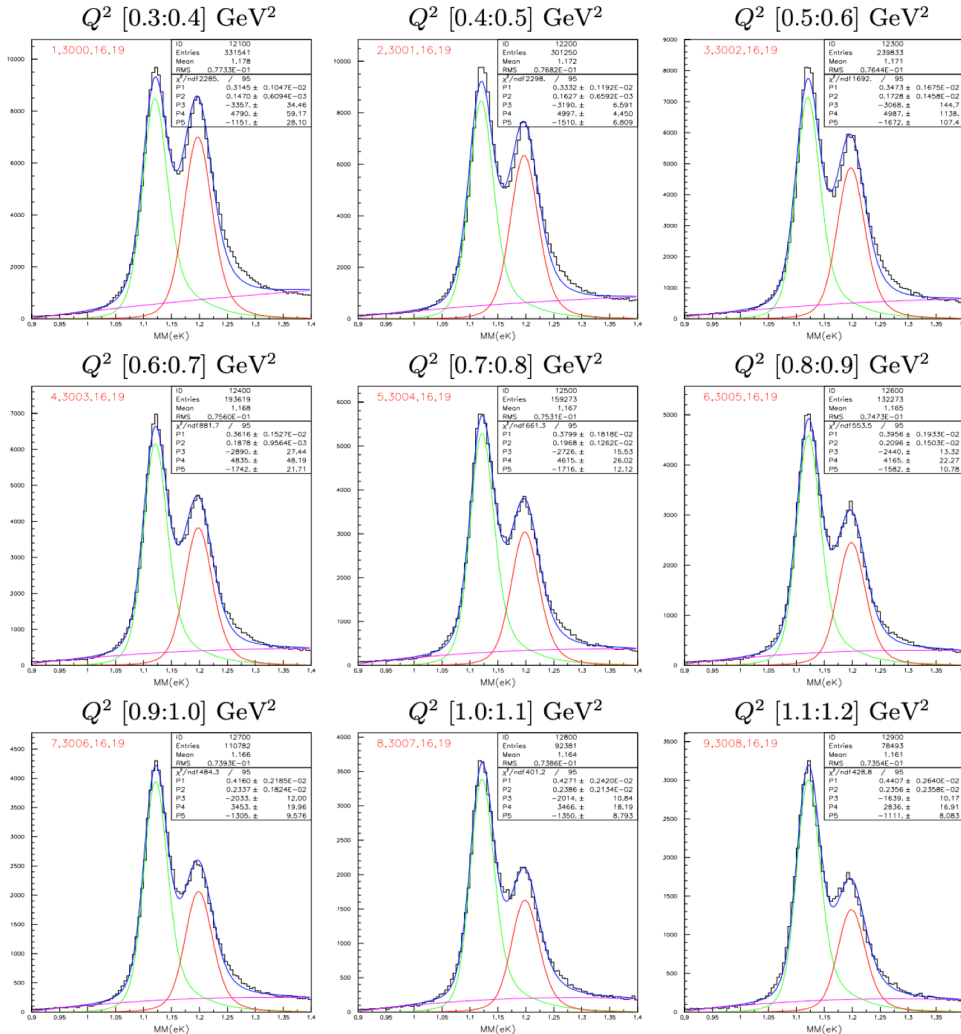
[https://clasweb.jlab.org/wiki/index.php/Run\\_Group\\_K#tab=KY\\_Analysis\\_Work](https://clasweb.jlab.org/wiki/index.php/Run_Group_K#tab=KY_Analysis_Work)



Backup Slides

# MM Spectrum Fits

RG-K 6.5 GeV MM fits, sum over  $W$  and  $\cos\theta_K^*$ , P2 background



MM(e<sup>+</sup>K<sup>+</sup>) (GeV)

Example fits use P2 background

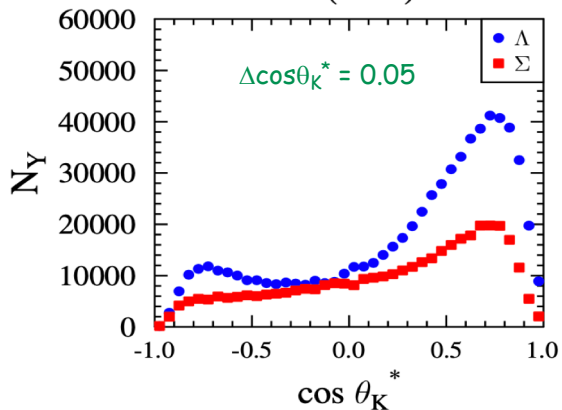
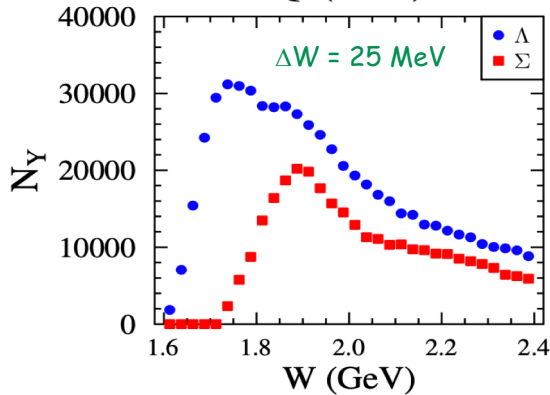
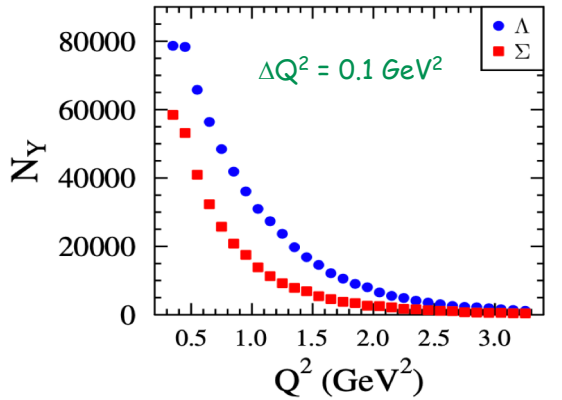
## Yield fitting approach:

- Generate Monte Carlo  $K^+\Lambda$  and  $K^+\Sigma^0$  samples to use as fitting templates in bins matched to the data:
  - *genKYandOnePion* with background merging
- The background can be modeled with a polynomial or with the background channel
  - $e^+\pi^+\pi^-\bar{p}$  - with  $\pi^+$  misidentified as a  $K^+$
- Fit function:
  - *GEMC* resolution is better than data, so fit uses a Gaussian convolution of the templates to minimize  $\chi^2$

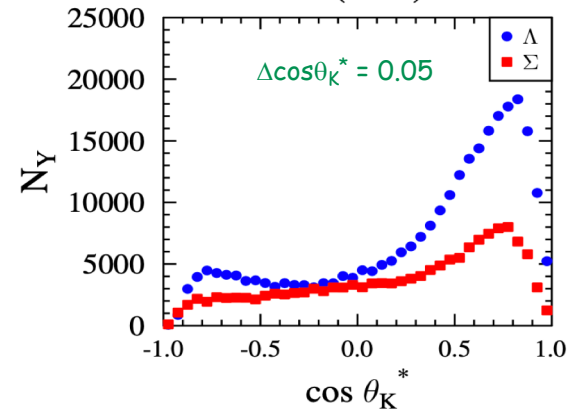
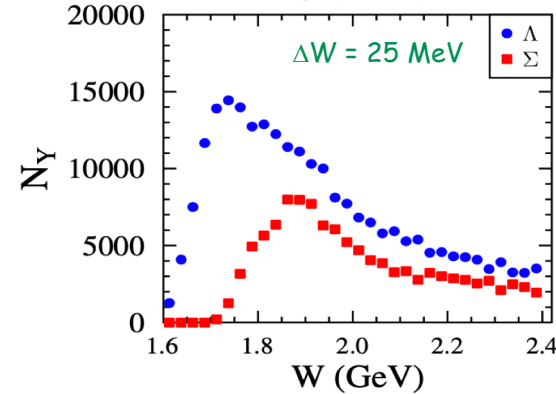
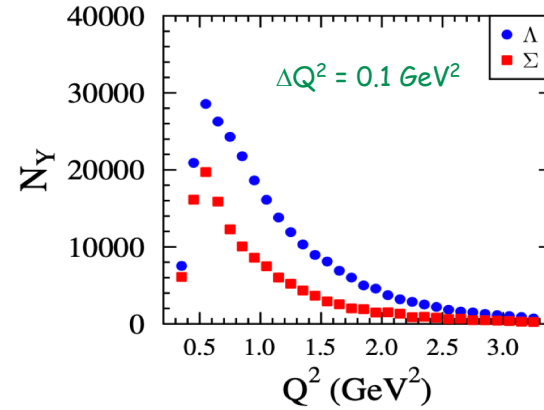
$$MM = A^*[TEMPLATE_\Lambda] + B^*[TEMPLATE_\Sigma] + C^*[bck]$$

# RG-K Hyperon Yields

6.5 GeV



7.5 GeV

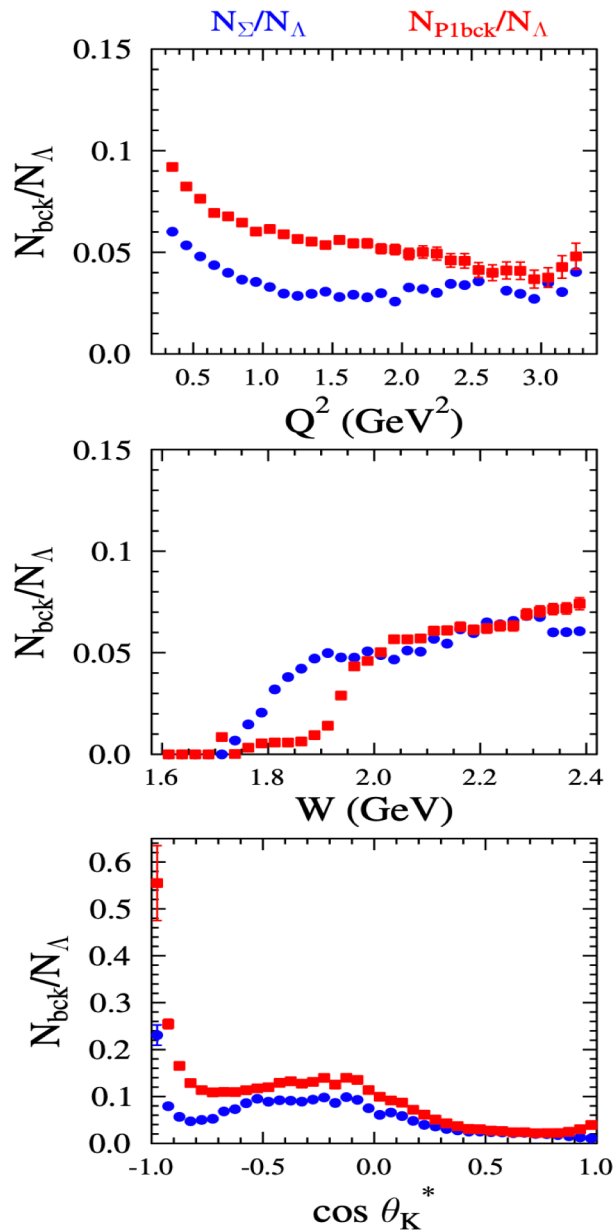


$N_{\Lambda} = 620k$   
 $N_{\Sigma} = 333k$

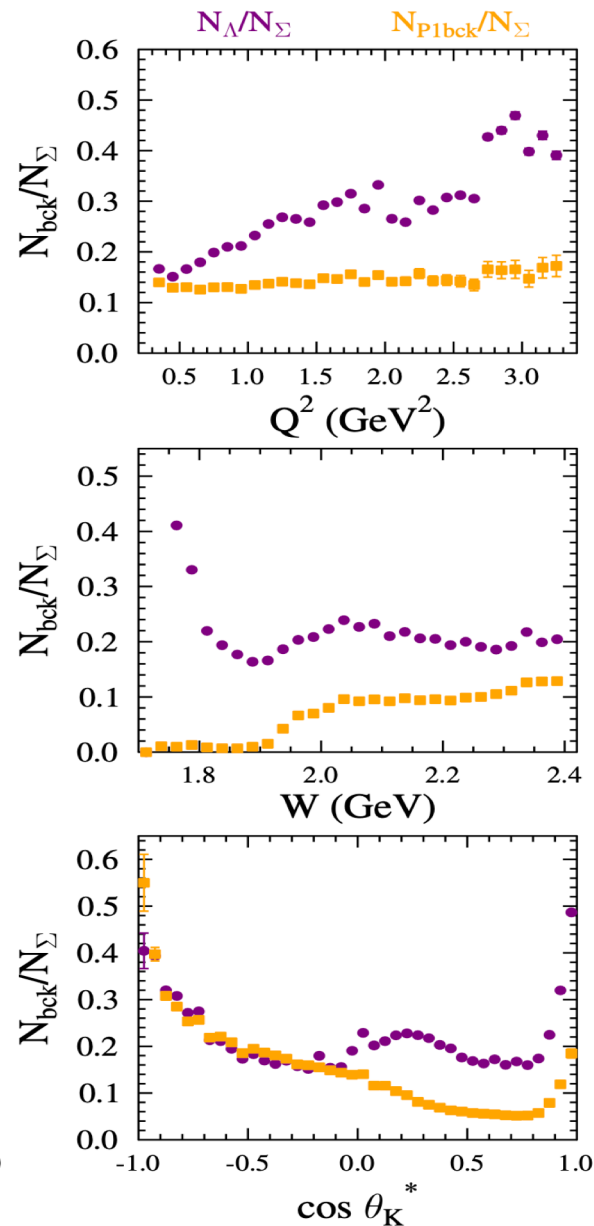
$N_{\Lambda} = 264k$   
 $N_{\Sigma} = 135k$

# Background Ratios

$\Lambda$  Mass Region



$\Sigma^0$  Mass Region



# RG-K KY Coordinate System

## 6.1 Response Functions

Table 21 shows which response functions survive for various polarization conditions of the incident electron, target proton, and recoiling hyperon. In total, of the possible 144 terms in the full expansion of eq.(5), only 36 independent, non-vanishing response functions are necessary to describe the electroproduction of pseudoscalar mesons. The remaining terms vanish due to CPT symmetry considerations, or are related to other response functions that do not vanish.

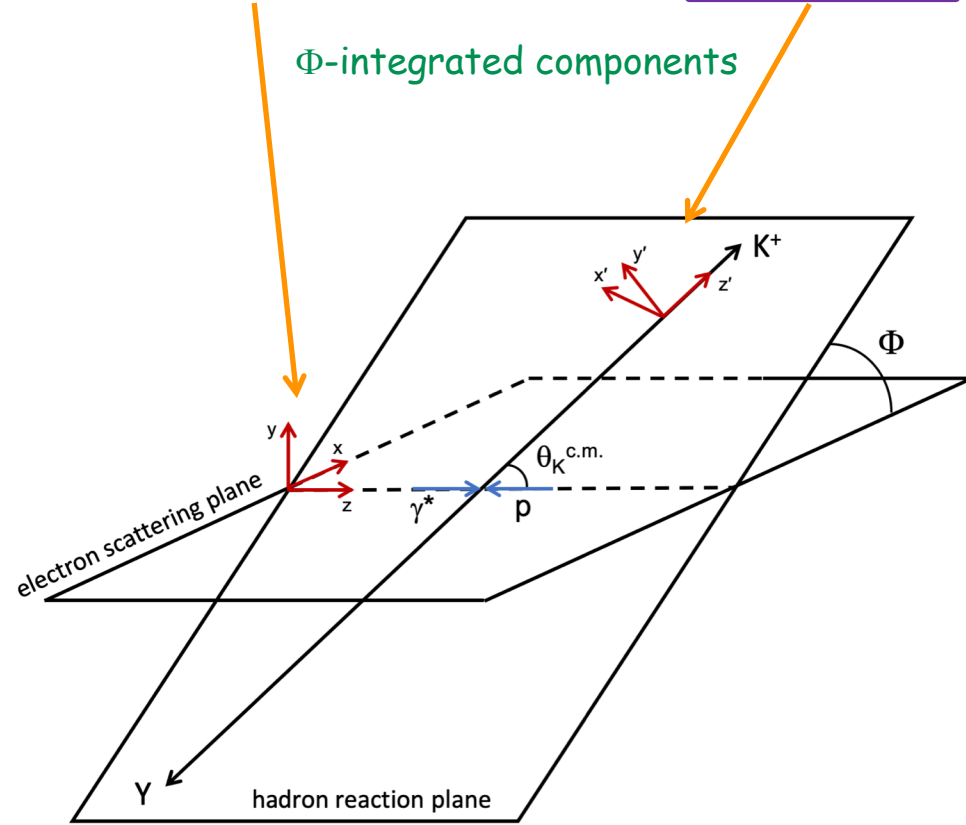
Pol.		Response Functions								
$\beta$	$\alpha$	T	L	${}^c$ LT	${}^s$ LT	${}^c$ TT	${}^s$ TT	${}^c$ LT'	${}^s$ LT'	TT'
0	0	$R_T^{00}$	$R_L^{00}$	$R_{LT}^{00}$	0	$R_{TT}^{00}$	0	0	$R_{LT'}^{00}$	0
$x'$	0	0	0	0	$R_{LT}^{x'0}$	0	$R_{TT}^{x'0}$	$R_{LT'}^{x'0}$	0	$R_{TT'}^{x'0}$
$y'$	0	$R_T^{y'0}$	$\ddagger$	$\ddagger$	0	$\ddagger$	0	0	$\ddagger$	0
$z'$	0	0	0	0	$R_{LT}^{z'0}$	0	$R_{TT}^{z'0}$	$R_{LT'}^{z'0}$	0	$R_{TT'}^{z'0}$
0	x	0	0	0	$R_{LT}^{0x}$	0	$R_{TT}^{0x}$	$R_{LT'}^{0x}$	0	$R_{TT'}^{0x}$
0	y	$R_T^{0y}$	$R_L^{0y}$	$R_{LT}^{0y}$	0	$\ddagger$	0	0	$R_{LT'}^{0y}$	0
0	z	0	0	0	$R_{LT}^{0z}$	0	$R_{TT}^{0z}$	$R_{LT'}^{0z}$	0	$R_{TT'}^{0z}$
$x'$	x	$R_T^{x'x}$	$R_L^{x'x}$	$R_{LT}^{x'x}$	0	$\ddagger$	0	0	$R_{LT'}^{x'x}$	0
$x'$	y	0	0	0	$\ddagger$	0	$\ddagger$	$\ddagger$	0	$\ddagger$
$x'$	z	$R_T^{x'z}$	$R_L^{x'z}$	$\ddagger$	0	$\ddagger$	0	0	$\ddagger$	0
$y'$	x	0	0	0	$\ddagger$	0	$\ddagger$	$\ddagger$	0	$\ddagger$
$y'$	y	$\ddagger$	$\ddagger$	$\ddagger$	0	$\ddagger$	0	0	$\ddagger$	0
$y'$	z	0	0	0	$\ddagger$	0	$\ddagger$	$\ddagger$	0	$\ddagger$
$z'$	x	$R_T^{z'x}$	$\ddagger$	$R_{LT}^{z'x}$	0	$\ddagger$	0	0	$R_{LT'}^{z'x}$	0
$z'$	y	0	0	0	$\ddagger$	0	$\ddagger$	$\ddagger$	0	$\ddagger$
$z'$	z	$R_T^{z'z}$	$\ddagger$	$\ddagger$	0	$\ddagger$	0	0	$\ddagger$	0

Table 21: Response functions for pseudoscalar meson production [7]. The target (recoil) polarization direction is indicated by  $\alpha$  ( $\beta$ ). The last three columns are for when the electron is polarized.  $\ddagger$  indicates a response function which does not vanish but is related to other response functions.

$$R^{\beta\alpha}(Q^2, W, \cos\theta_K^*)$$

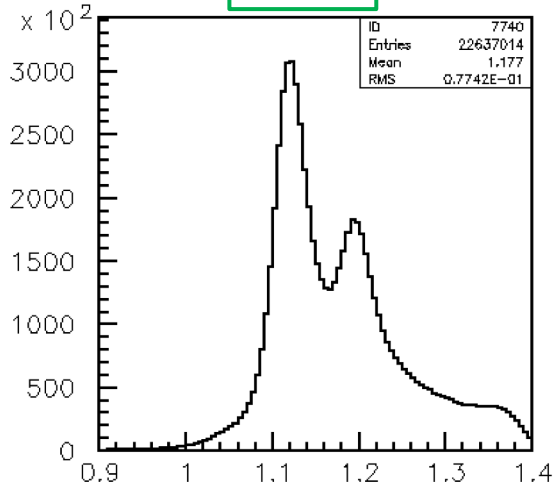
$P_x^0$	0
$P_y^0$	$\frac{1}{2}\sqrt{\epsilon(1+\epsilon)}K_I(R_{TL}^{x'0}\cos\theta_K^* + R_{TL}^{y'0} + R_{TL}^{z'0}\sin\theta_K^*)$
$P_z^0$	0
$P_x'$	$\frac{1}{2}\sqrt{\epsilon(1-\epsilon)}K_I(R_{TL}^{x'0}\cos\theta_K^* - R_{TL}^{y'0} + R_{TL}^{z'0}\sin\theta_K^*)$
$P_y'$	0
$P_z'$	$\sqrt{1-\epsilon^2}K_I(-R_{TL}^{x'0}\sin\theta_K^* + R_{TL}^{z'0}\cos\theta_K^*)$

$\mathcal{P}_{x'}^0$	0
$\mathcal{P}_{y'}^0$	$K_I(R_T^{y'0} + \epsilon R_L^{y'0})$
$\mathcal{P}_{z'}^0$	0
$\mathcal{P}_{x'}'$	$K_I\sqrt{1-\epsilon^2}R_{TT'}^{x'0}$
$\mathcal{P}_{y'}'$	0
$\mathcal{P}_{z'}'$	$K_I\sqrt{1-\epsilon^2}R_{TT'}^{z'0}$



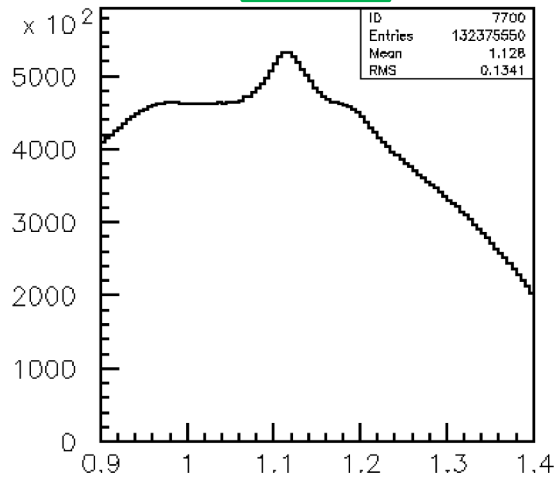
# RG-K Event Selection

$e'K^+_F$



MM(eK) Kf

$e'K^+_c$



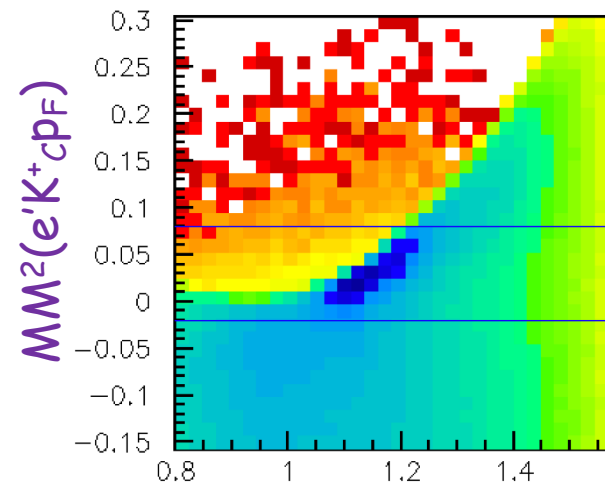
MM(eK) Kc

Clean-up of CD Events:

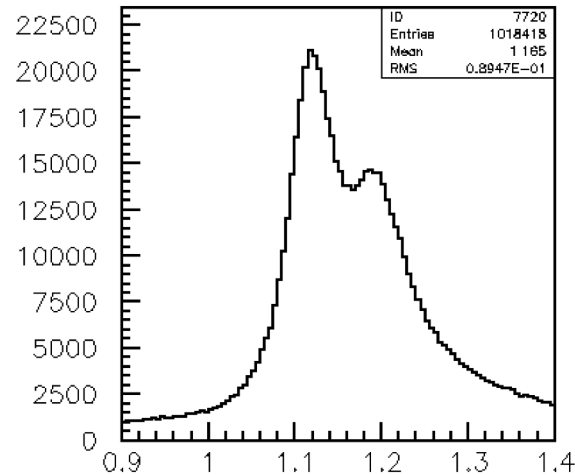
e.g.  $e'K^+_{cPF}$

Notes:

It is *absolutely essential* to include  $K^+_c$  in the analysis to access the kinematic range of relevance



$MM^2(e'K^+_c)$



MM(eK) Kc